SCIENCE CHINA
Information Sciences

• RESEARCH PAPER •

September 2019, Vol. 62 192205:1–192205:14
https://doi.org/10.1007/s11432-018-9759-9

Formation control with obstacle avoidance of second-order multi-agent systems under directed communication topology

Guoxing WEN[1,2*], C. L. Philip CHEN[2,4,5], Hui DOU[1], Hongli YANG[3] & Chunfang LIU[1]

[1]*College of Science, Binzhou University, Binzhou* 256600, *China;*
[2]*Department of Computer and Information Science, Faculty of Science and Technology, University of Macau, Macau* 999078, *China;*
[3]*Mathematics and Systems Science College, Shandong University of Science and Technology, Qingdao* 266590, *China;*
[4]*College of Navigation, Dalian Maritime University, Dalian* 116026, *China;*
[5]*State Key Laboratory of Management and Control for Complex Systems, Institute of Automation, Chinese Academy of Sciences, Beijing* 100080, *China*

Received 5 October 2018/Accepted 12 December 2018/Published online 26 July 2019

Abstract This paper addresses the obstacle avoidance problem of formation control for the multi-agent systems modeled by double integrator dynamics under a directed interconnection topology. The control task is finished by a leader-follower formation scheme combined with an artificial potential field (APF) method. The leader-follower scheme is carried out by taking the desired trajectory with the desired velocity as virtual leader, while the APF method is carried out by dealing with the obstacles as the high potential points. When the obstacle avoidance tasks are finished, the artificial potential forces degrade the formation performance, so their undesired effects are treated as disturbances, which is analyzed by the robust H_∞ performance. Based on Lyapunov stability theory, it is proved that the proposed formation approach can realize the control objective. The result is also extended to the switching multi-agent formation. The effectiveness of the proposed formation scheme is further confirmed by simulation studies.

Keywords formation control, obstacle avoidance, artificial potential field method, H_∞ performance, second-order multi-agent system, directed topology

Citation Wen G X, Chen C L P, Dou H, et al. Formation control with obstacle avoidance of second-order multi-agent systems under directed communication topology. Sci China Inf Sci, 2019, 62(9): 192205, https://doi.org/10.1007/s11432-018-9759-9

1 Introduction

Multi-agent systems are composed of multiple interacting intelligent individuals. By cooperation, the system can achieve many large-scale and difficult tasks, and surpass the capability of multiple individual agents. Owing to their excellent performances, such as flexibility, reliability, high efficiency, and extendibility to new capabilities, multi-agent systems are meeting the developing requirements of modern agriculture, industry and military. Moreover, the cost reduction and emergence of new technologies will facilitate the popularization of multi-agent techniques. To date, multi-agent systems have been widely applied in various areas, such as sensor networks, satellite clusters, coordination control of unmanned air vehicles, cooperation control of robot teams, and congestion control in communication networks [1–5].

* Corresponding author (email: wengx_sd@hotmail.com)

Multi-agent applications such as robot teams, autonomous vessels, and unmanned aircraft formations are usually driven by formation control [6–8], which finds the cooperative control algorithm or protocol that maintains the predefined formation pattern of the arriving agents. Formation control was originally inspired by social animal behaviors, such as fish schooling, bird flocking, and ant swarming. Over the past decades, several pioneer studies, such as the leader-follower strategy [9], virtual structure approach [10], behavior-based method [11], are continuously spreaded and quickly developed to derive a great number of results.

Recently, many multi-agent consensus approaches have been proposed [12–15]. Consensus control guides all agents towards a favorable agreement by information-sharing among the neighbors. With the development of multi-agent control, several excellent consensus methods have been extended to multi-agent formation. For example, multi-agent systems have been proposed for single integrated dynamics [16–19] and double integrated dynamics [20,21]. First-order multi-agent formation must only maintain a constant formation velocity, but the second-order case is more complex and requires difficult treatment of the time varying velocity.

As multi-agent formation must maintain a predefined shape, the interconnection topology for the information exchange plays an important role. Unfortunately, most of the research results focused on undirected communication topologies. Multi-agent formation is more challenging and realistic on directed topologies than on undirected topologies. On the one hand, the stability analysis and convergence proof are rendered complexly by the non-symmetric Laplacian matrix. On the other hand, directed topologies are common and general in real-world multi-agent engineering.

For multi-agent formation, obstacle avoidance is one of the most practical and challenging research topics. The objective can be fulfilled by the artificial potential field (APF) method, which was first proposed by Khatib [22], has been well developed because of their simplicity and efficiency. Its basic idea is to fill the working environment with a predefined APF. Recently, researchers have made many breakthroughs in multi-agent formation with APFs [23–25]. Wen et al. [23] applied the APF method to floating production storage and offloading-accommodation vessel systems for smooth gangway operation. In [24], APF method and behavior rule were combined for target tracking and obstacle avoidance. Zavlanos and Pappas [25] applied an artificial potential force that repels all agents from an undesired position, avoiding collisions among the agents.

It is well known that H_∞ techniques play a crucial role for system robustness all the time, and it has been well developed for the nonlinear and consensus control [26–29]. Its basic principle is that the gain of mapping between exogenous input and system output is less or no larger than the prescribed level. Recently, H_∞ techniques have been incorporated into several formation control schemes for obstacle avoidance [30,31]. Xue et al. [30] developed an H_∞ technique for formation of a hybrid multi-agent system. The H_∞ control is to reflect the attenuation level of obstacle avoidance for analyzing the negative effect on the formation. Meanwhile, Wen et al. [31] applied the APF method and H_∞ technique to stochastic multi-agent formation for obstacle-collision avoidance. However, all of these techniques were limited to the first-order multi-agent systems. The second-order formation control under directed topology remains unexplored thus far.

The paper addresses the obstacle avoidance problem of second-order multi-agent formation control with directed topology. The main contributions are summarized below:

(i) The obstacle avoidance problem in the multi-agent formation is solved by applying an APF method. To prove the theorem, a positive-definite function is found to satisfy $\dot{\nu}_{ij}(z_{ij}(t)) > 0$, where $z_{ij}(t)$ is the relative position variable between agent i and obstacle j.

(ii) The double integrator multi-agent formation containing a directed interconnection topology is developed. Because second-order multi-agent control considers both position and velocity, it is more practical and challenging than the first-order case.

(iii) By applying the H_∞ technique to multi-agent formation, we guarantee a highly robust system.

2 Preliminaries

2.1 System description

The multi-agent system of double integrator dynamics is described as

$$\dot{\chi}_i(t) = \nu_i(t), \quad \dot{\nu}_i(t) = u_i(t), \quad i = 1, 2, \ldots, n, \tag{1}$$

where $u_i(t) = [u_{i1}(t), \ldots, u_{im}(t)]^{\mathrm{T}} \in \mathbb{R}^m$ is the control variable; $\chi_i(t) = [\chi_{i1}(t), \ldots, \chi_{im}(t)]^{\mathrm{T}} \in \mathbb{R}^m$ and $\nu_i(t) = [\nu_{i1}(t), \ldots, \nu_{im}(t)]^{\mathrm{T}} \in \mathbb{R}^m$ are the position and velocity states, respectively.

The reference signals of the formation movement are given as

$$\dot{\chi}_r(t) = \nu_r(t), \quad \dot{\nu}_r(t) = f(\chi_r, \nu_r, t), \tag{2}$$

where $\chi_r(t) \in \mathbb{R}^m$ and $\nu_r(t) \in \mathbb{R}^m$ are position and velocity of the reference signals, and $f \in \mathbb{R}^m$ is a sufficiently smooth vector-valued function.

Assumption 1. $f \in L_2[0, t_h]$, $\forall t_h \in [0, \infty)$ in (2) is bounded by a constant ϵ, i.e., $\|f\| < \epsilon$, where $L_2[0, t_h]$ denotes square integrable function space such that $\int_0^{t_h} \|f\|^2 \mathrm{d}t < \infty$.

To steer the formation along the given route and velocity, leader-follower strategy is adopted in the control by taking the reference signal (2) as the virtual leader.

Definition 1 ([32])**.** Assume the initial states of multi-agent system (1) being bounded. If the solutions satisfy $\lim_{t\to\infty} \|\chi_i(t) - \chi_r(t) - \xi_i\| = 0$, $\lim_{t\to\infty} \|\nu_i(t) - \nu_r(t)\| = 0$, $i = 1, \ldots, n$, then the multi-agent formation is said to be achieved, where $\xi_i = [\xi_{i1}, \xi_{i2}, \ldots, \xi_{im}]^{\mathrm{T}}$ is the relative position vector between agent i and the reference signals (2), which describes the desired formation pattern.

Define the position and velocity tracking error variables as

$$e_{\chi i} = \chi_i(t) - \chi_r(t) - \xi_i, \quad e_{\nu i} = \nu_i(t) - \nu_r(t), \quad i = 1, \ldots, n, \tag{3}$$

where $e_{\chi i}(t)$ is with respect to position, $e_{\nu i}(t)$ is with respect to velocity.

Using dynamic equations (1) and (2), the following error dynamics are directly obtained:

$$\dot{e}_{\chi i}(t) = e_{\nu i}(t), \quad \dot{e}_{\nu i}(t) = u_i(t) - f(\chi_r, \nu_r, t), \quad i = 1, \ldots, n. \tag{4}$$

Rewrite the error dynamics (4) in compact form as

$$\dot{e}(t) = \left[\begin{bmatrix} 0_n & I_n \\ 0_n & 0_n \end{bmatrix} \otimes I_m \right] e(t) - \begin{bmatrix} 0_{nm} \\ F(t) \end{bmatrix} + \begin{bmatrix} 0_{nm} \\ u(t) \end{bmatrix}, \tag{5}$$

where $e(t) = [e_\chi^{\mathrm{T}}(t), e_\nu^{\mathrm{T}}(t)]^{\mathrm{T}}$, $e_\chi(t) = [e_{\chi 1}^{\mathrm{T}}(t), \ldots, e_{\chi n}^{\mathrm{T}}(t)]^{\mathrm{T}}$, $e_\nu(t) = [e_{\nu 1}^{\mathrm{T}}(t), \ldots, e_{\nu n}^{\mathrm{T}}(t)]^{\mathrm{T}}$, $F(t) = [f^{\mathrm{T}}, \ldots, f^{\mathrm{T}}]^{\mathrm{T}}$, $u(t) = [u_1^{\mathrm{T}}(t), \ldots, u_n^{\mathrm{T}}(t)]^{\mathrm{T}}$, 0_{nm} is an nm-dimensional zero vector, and $\otimes$ is Kronecker product.

Definition 2 (H_∞ performance [27])**.** Find the formation control $u(t)$ for the multi-agent system (1) such that the error variable $e(t) = [e_\chi^{\mathrm{T}}(t), e_\nu^{\mathrm{T}}(t)]^{\mathrm{T}}$ and bounded disturbance $\omega(t) \in L_2[0, t_h]$, $t_h \in [0, \infty)$ satisfy

$$\int_0^{t_h} \|e(t)\|^2 \mathrm{d}t \leqslant \gamma \int_0^{t_h} \|\omega(t)\|^2 \mathrm{d}t + V(0), \quad \omega(t) \in L_2[0, t_h], \tag{6}$$

where γ is a given positive constant, and $V(0)$ is the initial value of the system energy function $V(t)$.

The control objective. Design the H_∞ formation control protocol for which the multi-agent system (1) maintains the predefined formation patterns while moving along the desired trajectory at the desired velocity, and avoiding collision with obstacles.

Remark 1. The robust H_∞ control described in Definition 2 means that the impacts of disturbance $\omega(t)$ on the system states are attenuated to a desired level. If the system dynamics of (1) initializes with zero states, i.e., $V(0) = 0$, then the H_∞ performance (6) can be re-expressed as $\sup_{\omega \in L_2[0,t_h]} \frac{\int_0^{t_h} \|e(t)\|^2 \mathrm{d}t}{\int_0^{t_h} \|\omega(t)\|^2 \mathrm{d}t} \leqslant \gamma$. It implies that the gain between $e(t)$ and $\omega(t)$ is attenuated to the predefined level γ, i.e., the system states can be robust to the disturbances.

2.2 Algebraic graph theory

The communication graph of multi-agent system (1) is a strongly connected directed graph G containing n nodes. The node set, edge set, and adjacency matrix are denoted as $\Xi = \{\zeta_1, \zeta_2, \ldots, \zeta_n\}$, $\varepsilon \subseteq \Xi \times \Xi$, and $A = [a_{ij}]$; then the graph G can be represented as $G = (\Xi, \varepsilon, A)$. The edge $\varepsilon_{ij} = (\zeta_i, \zeta_j) \in \varepsilon$ if and only if information is communicated from node ζ_j to node ζ_i, where the node ζ_j is said being a neighbor of node ζ_i, and all neighbors of the node ζ_i are represented by the set $N_i = \{\zeta_j \in \Xi : \varepsilon_{ij} \in \varepsilon, j \neq i\}$. A directed network G is said strongly connected if there exits a directed path for any two distinct nodes ζ_i and ζ_j, i.e., (ζ_i, ζ_{i_1}), $(\zeta_{i_1}, \zeta_{i_2})$, $\ldots$,(ζ_{i_l}, ζ_j).

With respect to the edge ε_{ij}, the element a_{ij} of adjacency matrix A is valuated as $a_{ij} > 0 \Leftrightarrow \varepsilon_{ij} \in \varepsilon$, $a_{ij} = 0$ otherwise, and $a_{ii} = 0$. The communication weights between agents and the leader are described by $B = \mathrm{diag}\{b_1, \ldots, b_n\}$, where $b_i > 0$ if and only if agent i communicates with the leader, and $b_i = 0$ otherwise. It is assumed that at least an agent communicates with the leader, i.e., $b_1 + b_2 + \cdots + b_n > 0$.

Laplacian matrix L of the graph G can be generated as

$$L = C - A, \tag{7}$$

where $C = \mathrm{diag}\{c_1, c_2, \ldots, c_n\}$ and $c_i = \sum_{j=1}^{n} a_{ij}$. As all rows of the matrix sum to 0, 0 is an eigenvalue associating with eigenvector $\mathbf{1}_n = [1, 1, \ldots, 1]^{\mathrm{T}} \in \mathbb{R}^n$.

2.3 Artificial potential fields and repulsive forces

In the obstacle avoidance procedure, each obstacle is viewed as a high-potential point. If any agent is sufficiently close to an obstacle, the repulsive forces will be generated to push the multi-agent system away from the obstacle.

For agent i and obstacle k, define the relative position variate $z_{ik}(t)$ as

$$z_{ik}(t) = \chi_i(t) - o_k, \quad i = 1, \ldots, n, \quad k = 1, \ldots, q, \tag{8}$$

where $o_k \in \mathbb{R}^m$ denotes the kth obstacle.

From the system dynamics of (1), time derivative of $z_{ij}(t)$ is generated as

$$\dot{z}_{ik}(t) = \nu_i(t), \quad \dot{\nu}_i(t) = u_i(t), \quad i = 1, \ldots, n, \quad k = 1, \ldots, q. \tag{9}$$

The repulsive potential functions are defined below.

Definition 3 ([33])**.** A repulsive potential function associated with obstacle k is a nonnegative and differentiable function $\Psi_k(\|z_{ik}(t)\|)$ satisfying the following conditions:

(a) When $\|z_{ik}\| \leqslant \bar{d}_k$, the valid repulsion potential is triggered, and when $\|z_{ik}\| \to \underline{d}_k$, $\Psi_k(\|z_{ik}\|) \to +\infty$, where $\bar{d}_k$ is the distance threshold, $\underline{d}_k$ is the minimal separation distance from the obstacle k, and $\bar{d}_k > \underline{d}_k$.

(b) When $\|z_{ik}\| > \bar{d}_k$, $\Psi_k(\|z_{ik}\|)$ is weakened.

The repulsive force $\psi_{ik}(t)$ is generated from the negative gradient of $\Psi_k(\|z_{ik}\|)$ as

$$\psi_{ik}(t) = -\nabla_{z_{ik}} \Psi_k(\|z_{ik}\|), \quad k = 1, \ldots, q, \tag{10}$$

where $\nabla_{z_{ik}} \Psi_k(\|z_{ik}\|)$ denotes the gradient with respect to the relative position variable z_{ik}.

Because $\frac{\partial z_{ik}}{\partial \chi_i} = I_m$, the repulsive force term $\psi_{ik}(t)$ can also be expressed as

$$\psi_{ik}(t) = -\nabla_{\chi_i} \Psi_k(\|z_{ik}\|), \quad k = 1, \ldots, q, \tag{11}$$

where $\nabla_{\chi_i} \Psi_k(\|z_{ik}\|)$ denotes the gradient with respect to the position state $\chi_i(t)$.

Remark 2. When $\chi_i \in \Omega_k$, where $\Omega_k = \{\chi_i | \|z_{ik}\| = \|\chi_i(t) - o_k\| \leqslant \bar{d}_k\}$ is a compact set, agent i moves into the area of possible collision with obstacle k. Then the repulsive force $\psi_{ik}(t)$ will be triggered to compel the agent to maintain a respectable distance from obstacle k, and thus the possible collisions with obstacles are avoided. When $\{\chi_1, \ldots, \chi_n\} \notin \Omega_k$, according to Definition 3, the corresponding repulsive forces $\psi_{ik}(t)$, $i = 1, \ldots, n$, are weakened, and $\psi_{ik}(t) \in L_2[0, t_h]$.

2.4 Supporting Lemmas

Lemma 1 ([34]). The directed graph G is irreducible if and only if its Laplacian matrix L is strongly connected.

Lemma 2 ([35]). If a matrix $L = (l_{ij}) \in \mathbb{R}^{n\times n}$ has the following properties:

(a) $l_{ij} \leqslant 0$, $i \neq j$, $l_{ii} = -\sum_{j=1}^{n} l_{ij}$, $i = 1, 2, \ldots, n$, and

(b) The matrix L is irreducible,

then the following results can be obtained:

(1) There is a zero eigenvalue with multiplicity 1, and all nonzero eigenvalues have the positive real parts;

(2) $[1, \ldots, 1]^{\mathrm{T}}$ is a right eigenvector associated with eigenvalue 0;

(3) Let $\sigma = [\sigma_1, \ldots, \sigma_n]^{\mathrm{T}}$ be a normalized left eigenvector with respect to the eigenvalue 0. Then it can be chosen such that $\sigma_i > 0$ for all $i = 1, 2, \ldots, n$.

Lemma 3 ([36]). If the matrix $L = [l_{ij}] \in \mathbb{R}^{n\times n}$, where $l_{ij} = l_{ji} \leqslant 0$ for $i \neq j$ and $l_{ii} = -\sum_{j=1, i\neq j}^{n} l_{ij}$, is an irreducible matrix, then

$$L = \begin{bmatrix} l_{11} + b_1 & \cdots & l_{1n} \\ \vdots & \ddots & \vdots \\ l_{n1} & \cdots & l_{nn} + b_n \end{bmatrix}$$

is a positive definite matrix, where $b_1, b_2, \ldots, b_n$ are nonnegative constants to satisfy $b_1 + b_2 + \cdots + b_n > 0$.

Lemma 4 ([36]). The inequality $\left[\begin{smallmatrix} Q(x) & N(x) \\ N^{\mathrm{T}}(x) & P(x) \end{smallmatrix}\right] > 0$ holds if and only if either of the following inequalities hold:

(a) $Q(x) > 0$, $P(x) - N^{\mathrm{T}}(x)Q^{-1}(x)N(x) > 0$;

(b) $P(x) > 0$, $Q(x) - N(x)P^{-1}(x)N^{\mathrm{T}}(x) > 0$, where $Q(x) = Q^{\mathrm{T}}(x)$, $P(x) = P^{\mathrm{T}}(x)$.

Lemma 5 ([36]). $L(t) \in \mathbb{R}$ is a positive function with bounded initial value $L(0)$. If $\dot{L}(t) < -aL(t) + c$ is satisfied, where a, $c > 0$ are two constants, then the following inequality holds:

$$L(t) < \mathrm{e}^{-at}L(0) + \frac{c}{a}(1 - \mathrm{e}^{-at}).$$

Lemma 6. $L(t) \in \mathbb{R}$ is a positive definite continuous function with bounded initial value $L(0)$. If it holds that $\dot{L}(t) > bL(t)$ (or $\dot{L}(t) \leqslant bL(t)$) for $t \geqslant t_0$, where b is a positive constant, then we have

$$L(t) > \mathrm{e}^{b(t-t_0)}L(t_0) \text{ (or } L(t) \leqslant \mathrm{e}^{b(t-t_0)}L(t_0)). \tag{12}$$

Proof. From the fact $\dot{L}(t) > bL(t)$ (or $\dot{L}(t) \leqslant bL(t)$), the following result can be obtained:

$$\frac{\dot{L}(t)}{L(t)} > b \left(\text{or } \frac{\dot{L}(t)}{L(t)} \leqslant b\right).$$

Integrating the above inequality from t to t_0 yields

$$\ln(L(t))|_{t_0}^{t} > b(t - t_0) \text{ (or } \ln(L(t))|_{t_0}^{t} \leqslant b(t - t_0)). \tag{13}$$

Calculate the exponent on both sides of (13) and perform some simple manipulations. Then the inequality (12) can be obtained.

3 Main results

3.1 Fixed formation control

Define the formation errors concerning position and velocity as

$$\eta_{\chi i}(t) = \sum_{j\in N_i} a_{ij}(\chi_i(t) - \xi_i - \chi_j(t) + \xi_j) + b_i(\chi_i - \chi_r - \xi_i),$$

$$\eta_{\nu i}(t) = \sum_{j\in N_i} a_{ij}(\nu_i(t) - \nu_j(t)) + b_i(\nu_i(t) - \nu_r(t)),$$
$$i = 1, 2, \ldots, n, \tag{14}$$

where a_{ij} and b_i are the communication weights of agent i connected to neighbor agent j and the leader, respectively, which are associated with the adjacency matrices A and B (defined in Subsection 2.2).

Using the error variables defined in (3), the two coupling terms, $\eta_{\chi i}(t)$ and $\eta_{\nu i}(t)$, can be re-described as follows:

$$\eta_{\chi i}(t) = \sum_{j\in N_i} a_{ij}(e_{\chi i}(t) - e_{\chi j}(t)) + b_i e_{\chi i}(t),$$
$$\eta_{\nu i}(t) = \sum_{j\in N_i} a_{ij}(e_{\nu i}(t) - e_{\nu j}(t)) + b_i e_{\nu i}(t),$$
$$i = 1, 2, \ldots, n. \tag{15}$$

Design the distributed formation controller for the system (1) as follows:

$$u_i(t) = -\alpha(\eta_{\chi i}(t) + \eta_{\nu i}(t)) - \sum_{k=1}^{q} \beta_k \psi_{ik}(z_{ik}), \quad i = 1, 2, \ldots, n, \quad k = 1, 2, \ldots, q, \tag{16}$$

where $\alpha > 0$ and $\beta_k > 0$ are two design constants.

Remark 3. In the formation control (16), the graph-based coupling terms $-\alpha(\eta_{\chi i}(t)+\eta_{\nu i}(t))$ is utilized to maintain the predefined formation patterns and follow the desired reference signals. The repulsive force term $-\sum_{k=1}^{q} \psi_{ik}(z_{ik})$ is utilized to achieve the obstacle avoidance. Because they are two conflicting terms in non-obstacle environment, H_∞ control strategy is applied for guaranteeing the system robustness.

By substituting (16) into (5) and (9), the following equations can be obtained:

$$\dot{e}(t) = -\left[\begin{bmatrix} 0_{n\times n} & -I_n \\ \alpha\tilde{L} & \alpha\tilde{L} \end{bmatrix} \otimes I_m\right] e(t) - \begin{bmatrix} 0_{nm} \\ \psi(t) \end{bmatrix} - \begin{bmatrix} 0_{nm} \\ F(t) \end{bmatrix}, \tag{17}$$

$$\dot{z}_{ij}(t) = \nu_i(t), \quad \dot{\nu}_i(t) = -\alpha\left(\eta_{\chi i} + \eta_{\nu i}\right) - \sum_{k=1}^{q} \beta_k \psi_{ik}\left(z_{ik}\right), \quad i = 1, 2, \ldots, n, \quad k = 1, \ldots, q, \tag{18}$$

where $\tilde{L} = L + B$, and $\psi(t) = [(\sum_{k=1}^{p} \beta_k \psi_{1k})^{\mathrm{T}}, \ldots, (\sum_{k=1}^{p} \beta_k \psi_{nk})^{\mathrm{T}}]^{\mathrm{T}}$.

In recent years, H_∞ robust techniques have been implemented in several consensus control methods, such as [28, 29]. In [28], the H_∞ consensus method for the first-order multi-agent with directed graph G is developed by transforming original system to the reduced-order form. Finally, the consensus and H_∞ robust performance are proven. In [29], the H_∞ consensus control is extended to the second-order system that contains parameter uncertainties and disturbances.

In [30, 31], H_∞ techniques are extended to multi-agent formation for the first-order system under undirected communication topology. Because of the coupling of position and velocity states, it is much difficult to analyze the system stability and error convergence for second-order multi-agent under the directed communication graph. The challenging work is addressed in this paper. The main conclusions are described by the following theorems.

Theorem 1. The multi-agent system (1) is with bounded initial states under the strongly connected graph G. If the following condition (19) for parameters α and β_k, $k = 1, \ldots, q$ holds, then the control objective can be achieved by the proposed formation protocol (16), i.e., the multi-agent system can maintain a predefined formation pattern following the desired route and velocity, while avoiding collision with obstacles.

$$\alpha > \frac{2\max_{1\leqslant i\leqslant n}(\sigma_i) + 1}{\lambda_{\min}(\Gamma)}, \quad \beta_k > 0, \tag{19}$$

where $\lambda_{\min}(\Gamma)$ is the minimum eigenvalue of matrix Γ, $\Gamma = \tilde{L}^{\mathrm{T}}\Delta + \Delta\tilde{L} = L^{\mathrm{T}}\Delta + \Delta L + 2\Delta B$, $\Delta = \mathrm{diag}\{\sigma_1, \sigma_2, \ldots, \sigma_n\}$, and $\sigma = [\sigma_1, \sigma_2, \ldots, \sigma_n]^{\mathrm{T}}$ with $\sigma_i > 0$ is the normalized left eigenvector of L associated with the eigenvalue 0 (Lemma 2).

Remark 4. The proof of Theorem 1 contains two parts. Part 1 proves the formation behaviors for the case of $\{\chi_1, \ldots, \chi_n\} \notin \bigcup_{k=1}^{q} \Omega_k$, where $\Omega_k = \{\chi_i \| \|z_{ik}\| \leqslant \bar{d}_k\}$ is a compact set, and part 2 proves the obstacle avoidance behaviors for the case of $\forall \chi_i \in \forall \Omega_j$.

The case of part 1 implies all agents move out the area of possible collision with obstacles. According to the definition of artificial potential function (Definition 3), the repulsive forces term $\sum_{k=1}^{q} \beta_k \psi_{ik}(z_{ik})$ attains to handled level, which implies $\sum_{k=1}^{q} \beta_k \psi_{ik}(z_{ik}) \in L_2[0, t_h]$. Therefore, the artificial repulsive forces can be treated as the disturbance inputs and be analyzed by the H_∞ performance (Definition 2).

The case of part 2 implies agent i moves into the area of possible collision with obstacles, and the repulsive forces $\sum_{k=1}^{q} \beta_k \psi_{ik}(z_{ik})$ will be triggered rapid growth to compel the multi-agent system away from the obstacles.

Proof. **Part 1.** The following function is considered as the Lyapunov function candidate:

$$V(t) = e^{\mathrm{T}}(t) \left(\begin{bmatrix} \alpha\Gamma & \Delta \\ \Delta & \Delta \end{bmatrix} \otimes I_m \right) e(t). \tag{20}$$

First, the function (20) can be positive definite if the condition (19) holds. It is proven as follows.

Because $\left[\begin{smallmatrix} \alpha\Gamma & \Delta \\ \Delta & \Delta \end{smallmatrix}\right]$ is a symmetric matrix, $\left[\begin{smallmatrix} \alpha\Gamma & \Delta \\ \Delta & \Delta \end{smallmatrix}\right] > 0$ is equivalent to $\alpha\Gamma - \Delta = \alpha(\tilde{L}^{\mathrm{T}}\Delta + \Delta\tilde{L}) - \Delta = \alpha(L^{\mathrm{T}}\Delta + \Delta L + 2\Delta B) - \Delta > 0$ in accordance with Lemma 4.

From the definitions of the matrices L and Δ, the following fact can be obtained:

$$(L^{\mathrm{T}}\Delta + \Delta L)\mathbf{1}_n = L^{\mathrm{T}}\sigma + \Delta L \mathbf{1}_n = 0, \tag{21}$$

which implies $L^{\mathrm{T}}\Delta + \Delta L$ is a zero row-sum matrix. According to Lemma 3, $\Gamma = L^{\mathrm{T}}\Delta + \Delta L + 2\Delta B$ is a positive definite matrix, and thus $\alpha\Gamma - \Delta > 0$ is guaranteed when the design constant α satisfies (19). Hence $V(t)$ is a positive definite function.

Taking the time derivative of $V(t)$ along with (17), we have

$$\begin{aligned} \dot{V}(t) = &- e^{\mathrm{T}}(t) \left(\left(\begin{bmatrix} 0_{n\times n} & -I_n \\ \alpha\tilde{L} & \alpha\tilde{L} \end{bmatrix}^{\mathrm{T}} \begin{bmatrix} \alpha\Gamma & \Delta \\ \Delta & \Delta \end{bmatrix} + \begin{bmatrix} \alpha\Gamma & \Delta \\ \Delta & \Delta \end{bmatrix} \begin{bmatrix} 0_{n\times n} & -I_n \\ \alpha\tilde{L} & \alpha\tilde{L} \end{bmatrix} \right) \otimes I_m \right) e(t) \\ &- 2e^{\mathrm{T}}(t) \left(\begin{bmatrix} \alpha\Gamma & \Delta \\ \Delta & \Delta \end{bmatrix} \otimes I_m \right) \begin{bmatrix} 0_{nm} \\ \psi + F(t) \end{bmatrix}. \end{aligned} \tag{22}$$

Using the following facts that

$$\begin{bmatrix} 0_{n\times n} & -I_n \\ \alpha\tilde{L} & \alpha\tilde{L} \end{bmatrix}^{\mathrm{T}} \begin{bmatrix} \alpha\Gamma & \Delta \\ \Delta & \Delta \end{bmatrix} + \begin{bmatrix} \alpha\Gamma & \Delta \\ \Delta & \Delta \end{bmatrix} \begin{bmatrix} 0_{n\times n} & -I_n \\ \alpha\tilde{L} & \alpha\tilde{L} \end{bmatrix} = \begin{bmatrix} \alpha\Gamma & 0_{n\times n} \\ 0_{n\times n} & \alpha\Gamma - 2\Delta \end{bmatrix}, \tag{23}$$

$$\begin{aligned} e^{\mathrm{T}}(t) \left(\begin{bmatrix} \alpha\Gamma & \Delta \\ \Delta & \Delta \end{bmatrix} \otimes I_m \right) \begin{bmatrix} 0_{nm} \\ \psi + F(t) \end{bmatrix} &= e_\chi^{\mathrm{T}}(t) \left(\Delta \otimes I_m\right) \left(\psi + F(t)\right) + e_\nu^{\mathrm{T}}(t) \left(\Delta \otimes I_m\right) \left(\psi + F(t)\right) \\ &= e^{\mathrm{T}}(t) \left(\begin{bmatrix} \Delta & 0_{n\times n} \\ 0_{n\times n} & \Delta \end{bmatrix} \otimes I_m \right) \begin{bmatrix} \psi(t) + F(t) \\ \psi(t) + F(t) \end{bmatrix}, \end{aligned} \tag{24}$$

Eq. (22) can be rewritten as

$$\dot{V}(t) = -e^{\mathrm{T}}(t) \left(\begin{bmatrix} \alpha\Gamma & 0_{n\times n} \\ 0_{n\times n} & \alpha\Gamma - 2\Delta \end{bmatrix} \otimes I_m \right) e(t) - 2e^{\mathrm{T}}(t) \left(\begin{bmatrix} \Delta & 0_{n\times n} \\ 0_{n\times n} & \Delta \end{bmatrix} \otimes I_m \right) \begin{bmatrix} \omega(t) \\ \omega(t) \end{bmatrix}, \tag{25}$$

where $\omega(t) = \psi(t) + F(t)$.

Adding and subtracting the term

$$\begin{bmatrix}\omega(t)\\ \omega(t)\end{bmatrix}^{\mathrm{T}}\left(\left(\begin{bmatrix}\Delta & 0_{n\times n}\\ 0_{n\times n} & \Delta\end{bmatrix}^{\mathrm{T}}\begin{bmatrix}\Delta & 0_{n\times n}\\ 0_{n\times n} & \Delta\end{bmatrix}\right)\otimes I_m\right)\begin{bmatrix}\omega(t)\\ \omega(t)\end{bmatrix}$$

on the right hand side of the inequality (25) yields

$$\begin{aligned}\dot{V}(t) =& -e^{\mathrm{T}}(t)\left(\begin{bmatrix}\alpha\Gamma - I_n & 0_{n\times n}\\ 0_{n\times n} & \alpha\Gamma - 2\Delta - I_n\end{bmatrix}\otimes I_m\right)e(t)\\ &-\left\|e(t) + \left(\begin{bmatrix}\Delta & 0_{n\times n}\\ 0_{n\times n} & \Delta\end{bmatrix}\otimes I_m\right)\begin{bmatrix}\omega(t)\\ \omega(t)\end{bmatrix}\right\|^2\\ &+\begin{bmatrix}\omega(t)\\ \omega(t)\end{bmatrix}^{\mathrm{T}}\left(\left[\begin{bmatrix}\Delta & 0_{n\times n}\\ 0_{n\times n} & \Delta\end{bmatrix}^{\mathrm{T}}\begin{bmatrix}\Delta & 0_{n\times n}\\ 0_{n\times n} & \Delta\end{bmatrix}\right]\otimes I_m\right)\begin{bmatrix}\omega(t)\\ \omega(t)\end{bmatrix}.\end{aligned}\tag{26}$$

Further, Eq. (26) can become the following one:

$$\dot{V}(t) < -e^{\mathrm{T}}(t)\left(\begin{bmatrix}\alpha\Gamma - I_n & 0_{n\times n}\\ 0_{n\times n} & \alpha\Gamma - 2\Delta - I_n\end{bmatrix}\otimes I_m\right)e(t) + \begin{bmatrix}\omega(t)\\ \omega(t)\end{bmatrix}^{\mathrm{T}}\left(\begin{bmatrix}\Delta^{\mathrm{T}}\Delta & 0_{n\times n}\\ 0_{n\times n} & \Delta^{\mathrm{T}}\Delta\end{bmatrix}\otimes I_m\right)\begin{bmatrix}\omega(t)\\ \omega(t)\end{bmatrix}.\tag{27}$$

By choosing the control parameter α to satisfy the condition (19), the matrix $\left[\begin{smallmatrix}\alpha\Gamma - I_n & 0_{n\times n}\\ 0_{n\times n} & \alpha\Gamma - 2\Delta - I_n\end{smallmatrix}\right]$ is positive definite. Let γ_1 be the minimum eigenvalue of the matrix $\left[\begin{smallmatrix}\alpha\Gamma - I_n & 0_{n\times n}\\ 0_{n\times n} & \alpha\Gamma - 2\Delta - I_n\end{smallmatrix}\right]$, and let γ_2 be the maximum eigenvalue of the matrix $\left[\begin{smallmatrix}\Delta^{\mathrm{T}}\Delta & 0_{n\times n}\\ 0_{n\times n} & \Delta^{\mathrm{T}}\Delta\end{smallmatrix}\right]$, i.e., $\gamma_2 = 2\max\{\sigma_1^2, \ldots, \sigma_n^2\}$. The inequality (27) can be rewritten as follows:

$$\dot{V}(t) < -\gamma_1\|e(t)\|^2 + \gamma_2\|\omega(t)\|^2.\tag{28}$$

Integrating the inequality (28) from $t = 0$ to $t = t_h$, we have

$$V(t_h) - V(0) < -\gamma_1\int_0^{t_h}\|e(t)\|^2\mathrm{d}t + \gamma_2\int_0^{t_h}\|\omega(t)\|^2\mathrm{d}t.\tag{29}$$

Based on $V(t_h) > 0$, rewrite the inequality (29) to the following one:

$$\int_0^{t_h}\|e(t)\|^2\mathrm{d}t < \frac{1}{\gamma_1}V(0) + \frac{\gamma_2}{\gamma_1}\int_0^{t_h}\|\omega(t)\|^2\mathrm{d}t.\tag{30}$$

From Assumption 1 and Definition 3, it can be concluded that $\omega(t) \in L_2[0, t_h]$ in this case. Therefore, the H_∞ performance (6) is satisfied, and it is proven that the proposed formation control method has good robustness.

After several simple manipulations, the inequality (28) can be rewritten as

$$\dot{V}(t) < -\gamma V(t) + \gamma_2\|\omega(t)\|^2,\tag{31}$$

where $\gamma = \gamma_1/\lambda_{\max}$, and $\lambda_{\max}$ is the maximum eigenvalue of matrix $\left[\begin{smallmatrix}\alpha\Gamma & \Delta\\ \Delta & \Delta\end{smallmatrix}\right]$.

From Assumption 1 and Definition 3, the term $\|\omega(t)\|^2$ can be bounded by a constant δ for this case, i.e., $\|\omega(t)\|^2 \leqslant \delta$. Further, the inequality (31) can become

$$\dot{V}(t) < -\gamma V(t) + \gamma_2\delta.\tag{32}$$

According to Lemma 5, the following inequality can be obtained based on (32).

$$V(t) < \mathrm{e}^{-\gamma t}V(0) + \frac{\gamma_2\delta}{\gamma}(1 - \mathrm{e}^{-\gamma t}).\tag{33}$$

Inequality (33) implies that $V(t)$ can reach a desired small range by choosing the appropriate design parameters. It means that the desired formation behavior can be obtained for the non-obstacle environment.

Part 2 (The collision avoidance behaviors are analyzed only for agent i and obstacle j)**.** Based on the relative position variable $z_{ij}(t)$, design an energy function:

$$V_{ij}(t) = \frac{1}{2} z_{ij}^{\mathrm{T}}(t) z_{ij}(t) + \frac{1}{2} \nu_i^{\mathrm{T}}(t) \nu_i(t). \tag{34}$$

Taking the time derivative of V_{ij} along with (18), we have

$$\dot{V}_{ij}(t) = z_{ij}^{\mathrm{T}}(t) \nu_i(t) - \alpha \nu_i^{\mathrm{T}}(t) \left(\eta_{\chi i}(t) + \eta_{\nu i}(t)\right) - \sum_{k=1, k \neq j}^{q} \beta_k \nu_i^{\mathrm{T}}(t) \psi_{ik}\left(z_{ik}\right) - \beta_j \nu_i^{\mathrm{T}}(t) \psi_{ij}\left(z_{ij}\right). \tag{35}$$

Because the dwell time of all agents is finite in the region of $\Omega_j = \{\chi_i | \|z_{ij}\| \leqslant \bar{d}_j\}$, these continuous terms $z_{ik}(t)$, $\nu_i(t)$, $\eta_{\chi i}(t)$, $\eta_{\nu i}(t)$ and $\sum_{k=1, k \neq j}^{q} \beta_k \nu_i^{\mathrm{T}}(t) \psi_{ik}(z_{ik})$ are bounded in the region. In addition, if agent i is close to obstacle j, the agent is moving along gradient direction of the artificial repulsive potential $\Psi_j(t)$. By Definition 3, $-\nu_i^{\mathrm{T}}(t) \psi_{ij}(t) = \nu_i^{\mathrm{T}} \nabla_{\chi_i} \Psi_j(t) \to +\infty$ if $\|z_{ij}\| \to \underline{d}_j$. Therefore, the following inequality is satisfied if agent i is close to obstacle k sufficiently:

$$\begin{aligned} -\nu_i^{\mathrm{T}}(t) \psi_{ij}(t) > & \frac{1}{2} z_{ij}^{\mathrm{T}}(t) z_{ij}(t) + \frac{1}{2} \nu_i^{\mathrm{T}}(t) \nu_i(t) - \frac{1}{\beta_j} z_{ij}^{\mathrm{T}}(t) \nu_i(t) \\ & + \frac{\alpha}{\beta_j} \nu_i^{\mathrm{T}}(t) \left(\eta_{\chi i}(t) + \eta_{\nu i}(t)\right) + \frac{1}{\beta_j} \sum_{k=1, k \neq j}^{q} \beta_k \nu_i^{\mathrm{T}}(t) \psi_{ik}\left(z_{ik}\right). \end{aligned} \tag{36}$$

Substituting (36) into (35), we have

$$\dot{V}_{ij}(t) > \beta_j V_{ij}. \tag{37}$$

According to Lemma 6, the following result can be obtained from (37):

$$z_{ij}^{\mathrm{T}}(t) z_{ij}(t) > 2\mathrm{e}^{\beta_j (t - t_0)} V_{ij}(t_0) - \nu_i^{\mathrm{T}}(t) \nu_i(t). \tag{38}$$

As the term $\nu_i^{\mathrm{T}}(t) \nu_i(t)$ is continuous, it is bounded in the compact set Ω_j. Therefore, by designing the parameter $\beta_j > 0$ large enough and setting appropriate initial positions, it can be guaranteed that $2\mathrm{e}^{\beta_j (t - t_0)} V_{ij}(t_0) - \nu_i^{\mathrm{T}}(t) \nu_i(t) > \underline{d}_j^2$, and that there exists $\|z_{ij}(t)\| > \underline{d}_j$, i.e., the multi-agent system can avoid collision with obstacles by the proposed formation control scheme.

3.2 Switching formation control

The proposed formation control scheme can also be extended to switching formation. Suppose that the whole process $[0, t_h]$ of the formation control is divided into a time sequence of uniformly bounded non-overlapping sub-processes: $[t_s, t_{s+1})$, $s = 1, \ldots, l$ with $t_1 = 0$, $t_{l+1} = t_h$, $t_{s+1} - t_s \geqslant \tau_0$, where τ_0 is called the minimal dwell time. In each time interval $[t_s, t_{s+1})$, formation pattern is fixed. For the convenience of analysis, a piecewise constant function $\varphi(t) : [0, t_h] \to \mathbb{M} = \{1, 2, \ldots, N\}$ is introduced, where N denotes the total number of all possible formation patterns. $\xi_i^{\varphi(t)} \in \mathbb{R}^m$ denotes the formation patterns at time t. The interconnection graph is assumed to be invariable.

For this case, the formation tracking error vectors are redefined as $e_{\chi i}^{\varphi}(t) = \chi_i(t) - \chi_r(t) - \xi_i^{\varphi(t)}$, $e_{\nu i}(t) = \nu_i(t) - \nu_r(t)$, and the error dynamics is

$$\dot{e}_{\chi i}^{\varphi}(t) = e_{\nu i}(t), \quad \dot{e}_{\nu i}(t) = u_i(t) - f, \quad i = 1, \ldots, n. \tag{39}$$

Then the formation errors become

$$\eta_{\chi i}^{\varphi}(t) = \sum_{j \in N_i} a_{ij} \left(e_{\chi i}^{\varphi}(t) - e_{\chi j}^{\varphi}(t)\right) + b_i e_{\chi i}^{\varphi},$$

$$\eta_{\nu i}(t) = \sum_{j\in N_i} a_{ij}\left(e_{\nu i}(t) - e_{\nu j}(t)\right) + b_i e_{\nu i}(t),$$
$$i = 1, 2, \ldots, n. \tag{40}$$

Using the above errors, the switching formation control for the time interval $[t_s, t_{s+1})$ is constructed as

$$u_i(t) = -\alpha\left(\eta^{\varphi}_{\chi i}(t) + \eta_{\nu i}(t)\right) - \sum_{k=1}^{q}\beta_k \psi_{ik}\left(z_{ik}\right), \quad i = 1, 2, \ldots, n. \tag{41}$$

The main conclusion is summarized by Theorem 2.

Theorem 2. Consider the multi-agent system (1) with the bounded initial states and switching formation pattern $\xi_i^{\varphi(t)}$ under the strongly connected graph G. If the design parameters α and β_k satisfy (19) and the minimal dwell time τ_0 is long enough, then the switching formation controller (41) can guarantee the multi-agent system to achieve the desired formation, while avoiding collision with obstacles.

Proof. Choose the following function as the common Lyapunov function for all time intervals:

$$V(t) = (e^{\varphi}(t))^{\mathrm{T}}\left(\begin{bmatrix}\alpha\Gamma & \Delta\\ \Delta & \Delta\end{bmatrix}\otimes I_m\right)e^{\varphi}(t), \tag{42}$$

where $e^{\varphi}(t) = [(e^{\varphi}_{\chi}(t))^{\mathrm{T}}, (e_{\nu}(t))^{\mathrm{T}}]^{\mathrm{T}}$, and $e^{\varphi}_{\chi}(t) = [(e^{\varphi}_{\chi 1}(t))^{\mathrm{T}}, \ldots, (e^{\varphi}_{\chi n}(t))^{\mathrm{T}}]^{\mathrm{T}}$.

Similar to the proof of Theorem 1, the time derivative of (42) for $t \in [t_s, t_{s+1})$ is

$$\dot{V}(t) < -\gamma_1\|e^{\varphi}(t)\|^2 + \gamma_2\|\omega(t)\|^2, \tag{43}$$

where $\gamma_1 = \lambda_{\min}([\begin{smallmatrix}\alpha\Gamma - I_n & 0\\ 0 & \alpha\Gamma - 2\Delta - I_n\end{smallmatrix}])$, $\gamma_2 = 2\max\{\sigma_1^2, \ldots, \sigma_n^2\}$.

Integrating (43) from t_s to t_{s+1}, we obtain

$$\int_{t_s}^{t_{s+1}}\left\|e^{\varphi}(t)\right\|^2 \mathrm{d}t < \frac{1}{\gamma_1}(V(t_s) - V(t_{s+1})) + \frac{\gamma_2}{\gamma_1}\int_{t_s}^{t_{s+1}}\left\|\omega(t)\right\|^2 \mathrm{d}t. \tag{44}$$

Furthermore, we have

$$\int_0^{t_h}\|e^{\varphi}(t)\|^2\mathrm{d}t = \sum_{s=1}^{l}\int_{t_s}^{t_{s+1}}\left\|e^{\varphi}(t)\right\|^2 \mathrm{d}t < \frac{1}{\gamma_1}V(0) + \frac{\gamma_2}{\gamma_1}\int_0^{t_h}\|\omega(t)\|^2\mathrm{d}t, \tag{45}$$

and then the H_∞ performance (6) is satisfied.

From (43), we obtain

$$\dot{V}(t) < -\gamma V(t) + \gamma_2\left\|\omega(t)\right\|^2, \tag{46}$$

where $\gamma = \gamma_1/\lambda_{\max}$, and $\lambda_{\max}$ is the maximum eigenvalue of matrix $[\begin{smallmatrix}\alpha\Gamma & \Delta\\ \Delta & \Delta\end{smallmatrix}]$.

Because $\|\omega(t)\|^2$ can be bounded by a constant δ, according to Lemma 5, the following inequality can be obtained:

$$V(t) < \mathrm{e}^{-\gamma(t-t_s)}V\left(t_s\right) + \frac{\gamma_2\delta}{\gamma}\left(1 - \mathrm{e}^{-\gamma(t-t_s)}\right). \tag{47}$$

From (47), the formation tracking error $e(t)$ can arrive the desired accuracy by designing the minimal dwell time τ_0 large enough.

It had been proven that a switched system is stable if it is stabilized in all individual intervals and the dwell time is sufficiently long [37], so stability can be guaranteed for the whole control process by the proposed formation control protocol.

The proof of the obstacle avoidance control is similar to the proof of Theorem 1.

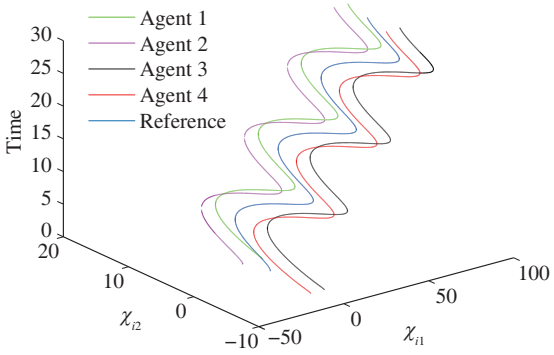

Figure 1 (Color online) The formation behavior in non-obstacle environment.

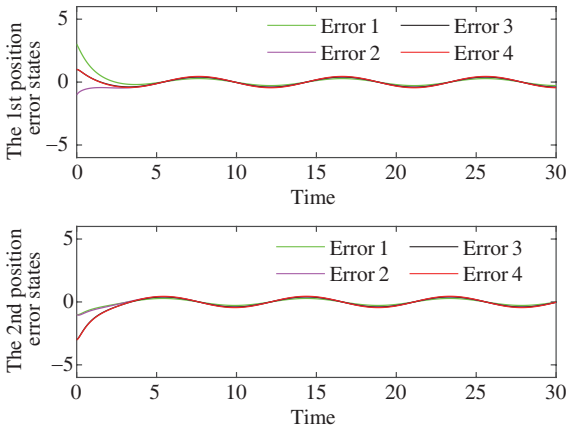

Figure 2 (Color online) The position tracking errors in non-obstacle environment.

4 Simulation examples

In this section, a numerical multi-agent instance is implemented for demonstrating effectiveness of the proposed formation scheme. In this instance, the multi-agent system has four agents and they move on the 2-D plane. The initial states are designed as $\chi_1(0) = [5.5, 4.8]^{\mathrm{T}}$, $\chi_2(0) = [-3.9, 5.2]^{\mathrm{T}}$, $\chi_3(0) = [5.6, -4.6]^{\mathrm{T}}$, $\chi_4(0) = [-4.6, -5.6]^{\mathrm{T}}$ and $\nu_{i=1,2,3,4}(0) = [1, 1]^{\mathrm{T}}$.

The desired reference signal is

$$\dot{\chi}_r(t) = \nu_r(t), \quad \dot{\nu}_r(t) = \begin{bmatrix} 2\sin(0.7t) \\ 2\cos(0.7t) \end{bmatrix}, \tag{48}$$

with initial values of $\chi_r(0) = [-1.2, 1.3]^{\mathrm{T}}$, $\nu_r(0) = [0.8, 1]^{\mathrm{T}}$.

For the strongly connected graph G, the adjacency matrix A and Laplacian matrix L are given as

$$A = \begin{bmatrix} 0 & 0.5 & 0 & 0.8 \\ 0.6 & 0 & 0.8 & 0 \\ 0.8 & 0 & 0 & 0.9 \\ 0 & 0.7 & 0.9 & 0 \end{bmatrix}, \quad L = \begin{bmatrix} 1.3 & -0.5 & 0 & -0.8 \\ -0.6 & 1.4 & -0.8 & 0 \\ -0.8 & 0 & 1.7 & -0.9 \\ 0 & -0.7 & -0.9 & 1.6 \end{bmatrix}.$$

The connection weight matrix between agents and the leader is $B = \mathrm{diag}\{1, 0, 0, 0\}$.

The potential functions are specified as

$$\Psi_k(\|z_{ik}\|) = \|z_{ik}\| \mathrm{e}^{(\|z_{ik}\|-4)^{-2}}, \quad k = 1, 2. \tag{49}$$

The potential repulsive forces derived from the negative gradient are

$$\begin{aligned} \psi_{ik}(\|z_{ik}\|) &= -\nabla_{z_{ik}} \Psi_{ik}(\|z_{ik}\|) \\ &= -\left(\|z_{ik}\|^{-1} \mathrm{e}^{(\|z_{ik}\|-4)^{-2}} - 2(\|z_{ik}\|-4)^{-3} \mathrm{e}^{(\|z_{ik}\|-4)^{-2}} \right) (\chi_i - o_k), \\ i &= 1, 2, 3, 4, \quad k = 1, 2. \end{aligned} \tag{50}$$

4.1 Formation control with fixed pattern

In this case, the formation patterns are described as $\xi_1 = [4.5; 4.5]^{\mathrm{T}}$, $\xi_2 = [-4.5; 4.5]^{\mathrm{T}}$, $\xi_3 = [4.5; -4.5]^{\mathrm{T}}$, $\xi_4 = [-4.5; -4.5]^{\mathrm{T}}$. There are two obstacles o_1 and o_2 located at $t = 5$ and $t = 15$, respectively. Figures 1–4 show the formation control performances. Figure 1 shows the multi-agent formation for the non-obstacle case, with the control parameter $\alpha = 50$. Figures 2 and 3 show the tracking errors with

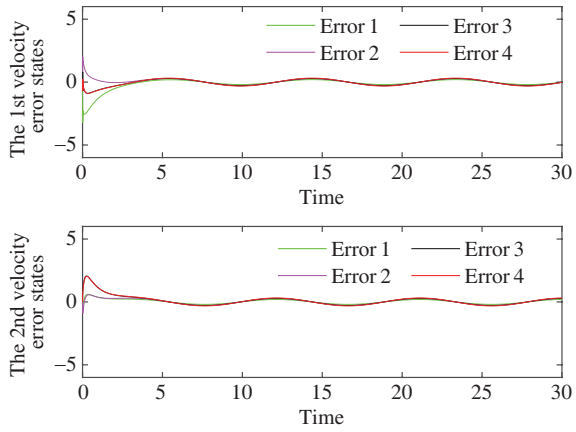

Figure 3 (Color online) The velocity tracking errors in non-obstacle environment.

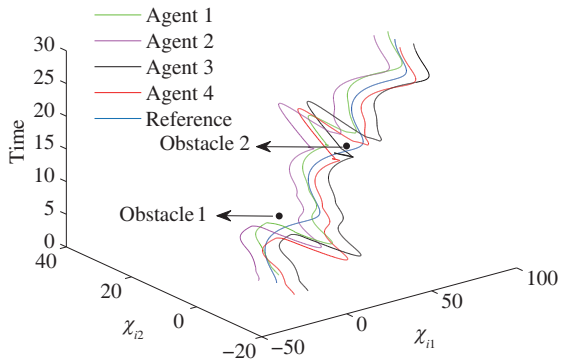

Figure 4 (Color online) The formation with obstacle avoidance behavior.

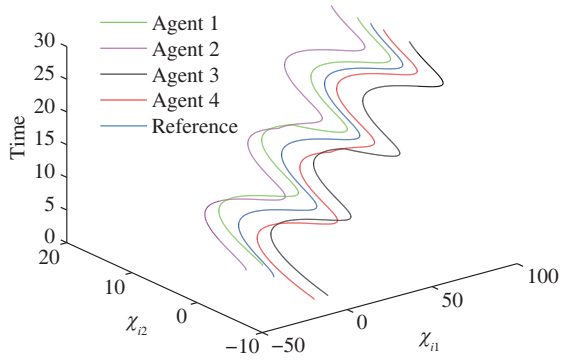

Figure 5 (Color online) The switching formation behavior in non-obstacle environment.

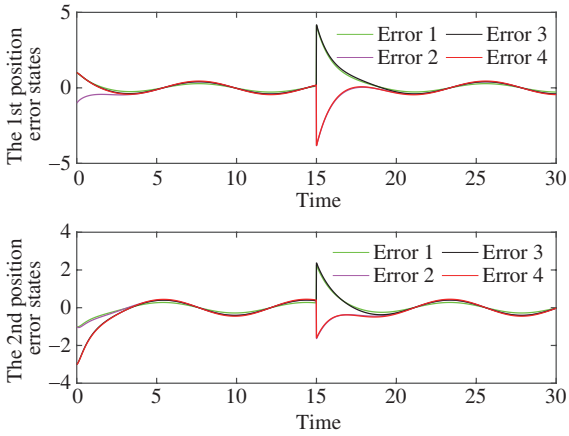

Figure 6 (Color online) The position errors of switching formation in non-obstacle environment.

respect to the position and velocity, respectively. Figure 4 displays the formation control results for obstacle environment, with the control parameters $\alpha = 27$, $\beta_1 = 18$, $\beta_2 = 32$. Figures 1–4 comfirms the performance of the proposed formation approach.

4.2 Formation control with switching shapes

In this case, the switching formation is performed by variating the formation patterns in two time intervals: $[0, 15)$ and $[15, 30]$. The formation pattern in the time interval $[0, 15)$ is $\xi_1^1 = [4; 4]^{\mathrm{T}}$, $\xi_2^1 = [-4; 4]^{\mathrm{T}}$, $\xi_3^1 = [4; -4]^{\mathrm{T}}$, $\xi_4^1 = [-4; -4]^{\mathrm{T}}$, and in the time interval $[15, 30]$ it is $\xi_1^2 = [0; 2]^{\mathrm{T}}$, $\xi_2^2 = [0; 6]^{\mathrm{T}}$, $\xi_3^2 = [0; -6]^{\mathrm{T}}$, $\xi_4^2 = [0; -2]^{\mathrm{T}}$. Two obstacle points are located at $t = 5$ and $t = 20$, respectively.

Figures 5–8 show the formation performances of the proposed scheme. Figure 5 shows the switching formation performance in the non-obstacle environment, with the control parameter $\alpha = 50$. Figures 6 and 7 show the position and velocity errors between agents and the reference signal, respectively. The switching formation performance of obstacle environment is shown in Figure 8, where the design parameters of the switching controller (41) are $\alpha = 49$, $\beta_1 = 23$, $\beta_2 = 15$. Figures 5–8 further demonstrate that the control objective can be achieved using the proposed control protocol (41).

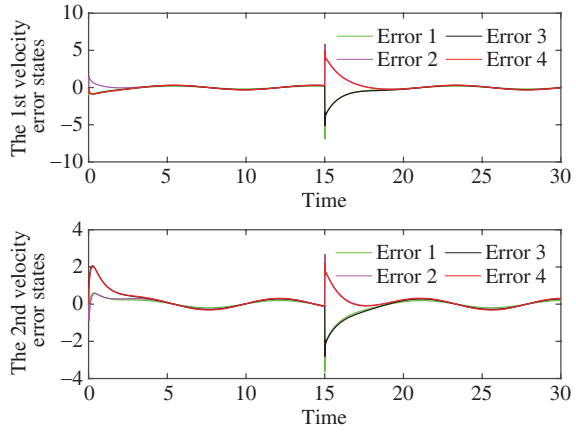

Figure 7 (Color online) The velocity errors of switching formation in non-obstacle environment.

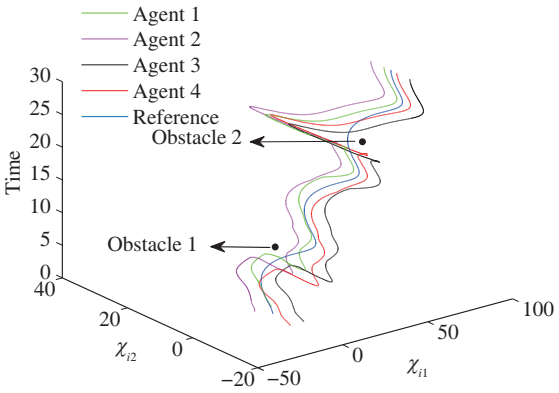

Figure 8 (Color online) The switching formation with obstacle avoidance behavior.

5 Conclusion

In the paper, a second-order formation of the multi-agent system under directed topology was proposed to solve the obstacle avoidance problem by using APF method. The obstacle avoidance problem was solved by employing the repulsive potential forces, which compelled the agents keeping off these obstacles, and the H_∞ method was utilized to analyze the unwanted potential effect. Then, the proposed control approach was proven that it can steer the multi-agent system to maintain the predefined formation patterns moving along with the desired route and velocity, meanwhile, avoiding collision with obstacles. Finally, a numerical instance was implemented and the desired results were shown. The future work will extent the study to nonlinear multi-agent systems by using neural networks or fuzzy logical systems, which have been applied in various classes of nonlinear systems, such as [38, 39].

Acknowledgements This work was supported in part by Shandong Provincial Natural Science Foundation (Grant Nos. ZR2018MF015, ZR2018MF023), in part by National Natural Science Foundation of China (Grant Nos. 61751202, 61572540), in part by Doctoral Scientific Research Staring Fund of Binzhou University (Grant No. 2016Y14). We would like to thank the mobility program of Shandong University of Science and Technology for the support in the work.

References

1 Yu W W, Chen G R, Wang Z D, et al. Distributed consensus filtering in sensor networks. IEEE Trans Syst Man Cybern B, 2009, 39: 1568–1577
2 Abdessameud A, Tayebi A. Attitude synchronization of a group of spacecraft without velocity measurements. IEEE Trans Autom Control, 2009, 54: 2642–2648
3 Hoffmann G M, Tomlin C J. Decentralized cooperative collision avoidance for acceleration constrained vehicles. In: Proceedings of Conference on Decision and Control, 2008. 4357–4363
4 Fua C H, Ge S S. COBOS: cooperative backoff adaptive scheme for multirobot task allocation. IEEE Trans Robot, 2005, 21: 1168–1178
5 Cui R, Ge S S, Ren B. Synchronized altitude tracking control of multiple unmanned helicopters. In: Proceedings of American Control Conference, 2010. 4433–4438
6 Abdessameud A, Tayebi A. Formation control of VTOL unmanned aerial vehicles with communication delays. Automatica, 2011, 47: 2383–2394
7 Ge S S, Fua C H, Lim K W. Multi-robot formations: queues and artificial potential trenches. In: Proceedings of IEEE International Conference on Robotics and Automation, 2004. 3345–3350
8 Cui R, Ge S S, How B V E, et al. Leader-follower formation control of underactuated autonomous underwater vehicles. Ocean Eng, 2010, 37: 1491–1502
9 Consolini L, Morbidi F, Prattichizzo D, et al. Leader-follower formation control of nonholonomic mobile robots with input constraints. Automatica, 2008, 44: 1343–1349
10 Lewis M A, Tan K H. High precision formation control of mobile robots using virtual structures. Auton Robot, 1997, 4: 387–403
11 Balch T, Arkin R C. Behavior-based formation control for multirobot teams. IEEE Trans Robot Autom, 1998, 14: 926–939

12 Wen G, Chen C L P, Liu Y J, et al. Neural network-based adaptive leader-following consensus control for a class of nonlinear multiagent state-delay systems. IEEE Trans Cybern, 2017, 47: 2151–2160
13 Ma C, Li T, Zhang J. Consensus control for leader-following multi-agent systems with measurement noises. J Syst Sci Complex, 2010, 23: 35–49
14 Liu J W, Huang J. Leader-following consensus of linear discrete-time multi-agent systems subject to jointly connected switching networks. Sci China Inf Sci, 2018, 61: 112208
15 Wang Z X, Fan J B, Jiang G P, et al. Consensus in nonlinear multi-agent systems with nonidentical nodes and sampled-data control. Sci China Inf Sci, 2018, 61: 122203
16 Ren W, Sorensen N. Distributed coordination architecture for multi-robot formation control. Robot Auton Syst, 2008, 56: 324–333
17 Xiao F, Wang L, Chen J, et al. Finite-time formation control for multi-agent systems. Automatica, 2009, 45: 2605–2611
18 Wen G, Chen C L P, Feng J, et al. Optimized multi-agent formation control based on an identifier-actor-critic reinforcement learning algorithm. IEEE Trans Fuzzy Syst, 2018, 26: 2719–2731
19 Wang C Y, Zuo Z Y, Gong Q H, et al. Formation control with disturbance rejection for a class of Lipschitz nonlinear systems. Sci China Inf Sci, 2017, 60: 070202
20 Liu C L, Tian Y P. Formation control of multi-agent systems with heterogeneous communication delays. Int J Syst Sci, 2009, 40: 627–636
21 Xie G, Wang L. Moving formation convergence of a group of mobile robots via decentralised information feedback. Int J Syst Sci, 2009, 40: 1019–1027
22 Khatib O. Real-time obstacle avoidance for manipulators and mobile robots. Int J Robot Res, 1986, 5: 90–98
23 Wen G, Ge S S, Tu F, et al. Artificial potential-based adaptive H_∞ synchronized tracking control for accommodation vessel. IEEE Trans Ind Electron, 2017, 64: 5640–5647
24 Yan J, Guan X P, Tan F X. Target tracking and obstacle avoidance for multi-agent systems. Int J Autom Comput, 2010, 7: 550–556
25 Zavlanos M M, Pappas G J. Potential fields for maintaining connectivity of mobile networks. IEEE Trans Robot, 2007, 23: 812–816
26 Chen B S, Lee C H, Chang Y C. H_∞ tracking design of uncertain nonlinear SISO systems: adaptive fuzzy approach. IEEE Trans Fuzzy Syst, 1996, 4: 32–43
27 Yang Y S, Zhou C J. Adaptive fuzzy H_∞ stabilization for strict-feedback canonical nonlinear systems via backstepping and small-gain approach. IEEE Trans Fuzzy Syst, 2005, 13: 104–114
28 Lin P, Jia Y, Li L. Distributed robust consensus control in directed networks of agents with time-delay. Syst Control Lett, 2008, 57: 643–653
29 Lin P, Jia Y. Robust H_∞ consensus analysis of a class of second-order multi-agent systems with uncertainty. IET Control Theory Appl, 2010, 4: 487–498
30 Xue D, Yao J, Wang J. H_∞ formation control and obstacle avoidance for hybrid multi-agent systems. J Appl Math, 2013, 2013: 1–11
31 Wen G, Chen C L P, Liu Y J. Formation control with obstacle avoidance for a class of stochastic multiagent systems. IEEE Trans Ind Electron, 2018, 65: 5847–5855
32 Wang J L, Wu H N. Leader-following formation control of multi-agent systems under fixed and switching topologies. Int J Control, 2012, 85: 695–705
33 Tanner H G, Jadbabaie A, Pappas G J. Stable flocking of mobile agents part I: dynamic topology. In: Proceedings of Conference on Decision and Control, 2003. 2016–2021
34 Chai W W. Synchronization in Complex Networks of Nonlinear Dynamical Systems. Singapore: World Scientific, 2007
35 Lu W, Chen T. New approach to synchronization analysis of linearly coupled ordinary differential systems. Phys D-Nonlinear Phenom, 2006, 213: 214–230
36 Liu Y J, Wen G X, Chen C L P, et al. Neural-network-based adaptive leader-following consensus control for second-order non-linear multi-agent systems. IET Control Theory Appl, 2015, 9: 1927–1934
37 Liberzon D. Switching in Systems and Control. Boston: Birkhäuser, 2003
38 Liu L, Liu Y J, Tong S C. Neural networks-based adaptive finite-time fault-tolerant control for a class of strict-feedback switched nonlinear systems. IEEE Trans Cybern, 2019, 49: 2536–2545
39 Liu L, Liu Y J, Tong S C. Fuzzy based multi-error constraint control for switched nonlinear systems and its applications. IEEE Trans Fuzzy Syst, 2018. doi: 10.1109/TFUZZ.2018.2882173